Structural determination of the polysaccharide isolated from biofilms produced by a clinical strain of *Klebsiella pneumoniae*

Paola Cescutti*, Gianluigi De Benedetto, Roberto Rizzo

Department of Life Sciences, University of Trieste, via L. Giorgieri 1, Bdg. C11, 34127 Trieste, Italy.

* Corresponding author. Department of Life Sciences, Bldg C11, University of Trieste, Via Licio Giorgieri 1, I-34127 Trieste, Italy. Tel.: +39 040 5588755.
E-mail address: pcescutti@units.it

Abstract

Klebsiella pneumoniae are Gram negative opportunistic pathogens producing capsular (K) polysaccharides. Seventy seven different K antigens have been described and they are the basis for K serotyping. Capsular polysaccharides are important virulence factors and have a relevant role for the structure of biofilm communities. Nevertheless, little information is available on the polysaccharides produced in biofilm matrices by *Klebsiella* spp. In the present study, a clinical isolate of *Klebsiella pneumoniae* was grown both on cellulose membranes deposited on agar plates, where it formed an adherent biofilm, and in liquid medium, where it formed floating biofilms (flocs). Extraction and purification of the polysaccharide fraction showed that only one main carbohydrate polymer was present in both adherent biofilms and flocs. Composition and linkage analysis, Smith degradation followed by ESI-MS, 1D and 2D NMR spectroscopy revealed that the polysaccharide belong to the type K24 and has the following structure:

$$[2)\text{-}\alpha\text{-D-Glc}p\text{A-}(1\rightarrow3)\text{-}\alpha\text{-D-Man}p\text{-}(1\rightarrow2)\text{-}\alpha\text{-D-Man}p\text{-}(1\rightarrow3)\text{-}\beta\text{-D-Glc}p\text{-}(1\rightarrow]_n$$

$$\begin{array}{c} 4 \\ \uparrow \\ 1 \\ \beta\text{-D-Man}p \end{array}$$

Keywords: *Klebsiella pneumoniae*; polysaccharide structure; biofilm; NMR; ESI-MS.

1. Introduction

Klebsiella pneumoniae are Gram negative opportunistic pathogens able to cause bacteremia, pneumonia, urinary tract and catheter-related infections, and community-acquired pyogenic liver abscess.[1] *K. pneumoniae* generally forms mucoid colonies because of the production of capsular (K) polysaccharides; seventy seven are the different K antigens synthesized by this species, but only some are known to be associated with human disease.[2,3] Serotyping is focussed on the K antigens because not only the number of different O antigens is limited to eight but also O serotyping is practically difficult to perform, due to the copious production of capsular polysaccharides masking the underlying lipopolysaccharides. K polysaccharides are also important virulence factors that confer resistance to phagocytosis and prevent killing of the bacteria by bactericidal serum factors.[4,5] Another virulence factor possessed by *K. pneumoniae* is the ability of forming biofilms, which are produced also *in vitro.* Despite the recognition that the capsule, together with the lipopolysaccharide, has an important role for the structure of biofilm communities,[5] little information is available on the polysaccharides excreted in biofilm matrices by *Klebsiella* spp..

In the present study, the clinical isolate *Klebsiella pneumoniae* Ts113 (KpTs113) was grown both on cellulose membranes deposited on agar plates, where it formed an adherent biofilm, and in liquid medium, where it formed floating biofilms (flocs).[6] The polysaccharide components were extracted from both matrices, purified and their structure determined mainly using NMR spectroscopy and ESI-MS of derived oligosaccharides.

2. Results and discussion

2.1. Purification and composition analysis of EPOL Kp113 obtained from biofilm developed on cellulose membranes

A rather large amount of biofilm matrix was obtained growing KpTs113 on cellulose membranes. About 15 mg of polysaccharide were recovered following purification and the sample was named **EPOL Kp113**. Composition analysis as alditol acetate derivatives revealed Man, Gal, and Glc in the molar ratios 1.94 : 0.29 : 1.00, while analysis of methyl-glycosides TMS derivatives, besides confirming the type and ratios of the neutral sugars, also showed the presence of GlcA (Man, Gal, Glc, GlcA in the molar ratios 2.19 : 0.31 : 1.00 : 0.22). The relative molar ratio of GlcA lower than 1 is

likely due to the more acid resistant characteristic of the glycosidic bond engaged by uronic acids. The absolute configuration was established to be D for all residues. The position of the glycosidic linkages was determined by GLC and GLC-MS analysis after derivatization of the sugar components to partially methylated alditol acetates. GLC analysis on a HP-1 column showed four peaks attributed to terminal Man, 2-linked Man co-eluting with 3-linked Glc,[7] 3-linked Man, and 3-linked Gal; integration of the respective peak areas gave the following relative molar ratio: 1.00 : 2.00 : 0.50 : 0.25. In order to separate 2-linked Man from 3-linked Glc, GLC and GLC-MS were performed also on a SP-2330 column; again four peaks were detected and the components were identified as terminal Man, 3-linked Glc, 2-linked Man co-eluting with 3-linked Man,[7] and 3-linked Gal, in the relative molar ratios 1.00 : 1.20 : 2.30 : 0.70. Comparison of the above integration data generated on two separate columns suggested equimolar amounts of 2-Man, 3-Man and 3-Glc. **EPOL Kp113** eluted as a single broad peak after chromatographic separation on the Sephacryl S-300 column (Figure S1 in Supplementary data); the fractions from the central portion of the peak were pooled together, dialyzed and recovered after freeze-drying. Composition analysis as alditol acetate derivatives of this sample revealed Man : Gal : Glc in the relative molar ratios 3.30 : 0.06 : 1.00, thus suggesting that galactose is the component of another polysaccharide present in lesser amounts and that t-Man, 2-Man and 3-Man were present in equimolar amounts. Galactose might derive from the O chain of lipopolysaccharides, released as a consequence of cell-damage, as some *Klebsiella pneumoniae* O polysaccharides (i.e. O1 and O2a, 2a,c) consist of galactans.[8] Moreover, the presence of t-Man indicated a branched residue and since the neutral hexoses are linked in one position only, most likely the GlcA is the branched residue.

2.2. Characterisation of the oligosaccharides obtained from Smith degradation

The sample **KP113 SD**, obtained after Smith degradation of the **EPOL Kp113**, was separated on a Bio Gel P2 column to give five major peaks (Figure S2 in Supplementary data). Fractions belonging to the same peak were pooled together, desalted by dialysis and analysed by ESI-MS in the positive ion mode. From linkage analysis, 3-Man and 3-Glc are resistant to periodate oxidation, t-Man was expected to be completely oxidized, and 2-Man was expected to give a glycerol-type aglycon. ESI-MS mass spectrum of peak 3 showed pseudomolecular ions at *m/z* 687.2 and 703.2 corresponding to the Na^+ and K^+ adducts, respectively, of an oligosaccharide composed of two Hex, one HexA and an aglycon of 164 u, in place of the expected glycerol. This aglycon is most probably a 1,3-dioxolane formed by trans-acetylation during the hydrolytic step of the degradation;[9] the formation of this

derivative has been frequently reported arising from 2-linked residues.[10,11] Interpretation of the MS^2 spectrum of the parent ion at *m/z* 687.2 (Figure S3 in Supplementary data) determined the following sequence for the oligosaccharide: Hex-HexA-Hex-Dox (Dox = 1,3-dioxolane) (Table 1). ESI-MS of the permethylated oligosaccharide gave pseudomolecular ions at *m/z* 850.3 and 855.3 corresponding to the NH_4^+ and Na^+ adducts, respectively, and showed that 12 hydroxyl functions have been methylated, in agreement with the proposed oligosaccharide structure. MS^2 of the ion at *m/z* 855.3 and MS^3 of the ion at *m/z* 637.4 (Figure 1) not only confirmed the sequence deduced from the un-methylated oligosaccharide, but gave information on the glycosidic linkage engaged by the GlcA residue. In fact, the presence of the ion at *m/z* 315.3 ($^{1,3}A_2$),[12] arising from cross-ring cleavage of the GlcA residue, indicated that the hexose residue is 2-linked to the uronic acid residue.

2.3 NMR spectroscopy of EPOL Kp113

The ^{1}H NMR spectrum (Figure 2a) of a solution of **EPOL Kp113** showed five anomeric signals at 5.45, 5.44, 5.00, 4.69 and 4.65 ppm which were labelled from **A** to **E** in order of decreasing chemical shift. The signal **D** had a coupling constant $J_{H1,2}$ = 7.63 Hz, indicative of a β anomeric configuration. The anomeric configuration of the other anomeric resonances were determined by measuring their $J_{C1,H1}$, after recording a coupled HSQC experiment. The values found (Table 2) showed that the residues **A**, **B** and **C** have the α anomeric configuration, while the residues **D** and **E** have the β one.[13] Proton connectivities from H-1 to H-5 of residues **B**, **C**, **D**, and **E** were determined from the COSY (Figure S4 in Supplementary data) and TOCSY (Figure S5 in Supplementary data) spectra. Regarding residue **A**, H-2 was easily attributed in the COSY spectrum, while a 1D TOCSY (data not shown) was required to identify H-3 and H-4, through irradiation of H-2. In this way, most of the proton chemical shifts for each spin system were determined. An HSQC experiment (Figure 3) gave the corresponding ^{13}C chemical shifts, together with the assignment of H-5 and C-5 of spin system **A**. The obtained chemical shifts are reported in Table 2. By comparison of the experimental chemical shifts for each spin system with literature values[14], the type of monosaccharide together with the position of glycosidic linkages were determined. Residues **B** and **D** have chemical shifts values typical of the *gluco* configuration, while **A**, **C** and **E** those of the *manno* configuration. Therefore, it was deduced that **A** is 2-Man, **B** is 2,4-GlcA, **C** is 3-Man, **D** is 3-Glc and **E** is t-Man. NOESY plot (Figure 4, Table 3) showed intra-residues as well as the following inter-residues connectivities which established the sequence of the monosaccharides in the repeating unit: **A1** to **D3**, **B1** to **C3**, **C1** to **A2**, **D1** to **B2**, and

E1 to **B4**. The intra-residues connectivities of the mannose unities confirmed the anomeric configuration assignments: in fact, the spin system **E**, in the β anomeric configuration, was the only one to have n.o.e. contacts between H-1 and H-3 as well as H-5. An HMBC experiment gave the carbonyl chemical shift value of the GlcA residue and confirmed most of the inter-residue connectivities (Figure S6 in Supplementary data); the long range correlation of H-1 of **B** with C-3 of **C** was lacking, while the inter-residue correlation H-1 of **C** with C-2 of **A** was probably overlapping with the intra-residue one H-1 of **C** with C-3 of **C**. All the data collected established the following structure for **EPOL Kp113** repeating unit:

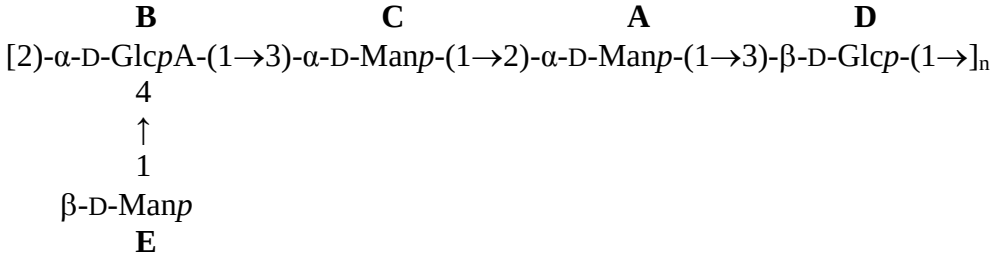

The CASPER computer program[15, 16] was used to evaluate the structure determined for the **EPOL Kp113** and to compare the experimental chemical shifts with those arising from the program output. ^{13}C and ^{1}H resonances deduced from the HSQC plot together with five $^{1}J_{C1,H1}$ values, the absolute configurations and the glycosidic linkages were submitted to the 'determine structure' module of the CASPER program. The calculation gave a list of the ten best possible structures, with the highest ranked corresponding to the sequence determined experimentally (Figure S7 in Supplementary data). Moreover, the chemical shifts assignment of each proton and carbon atoms matched the assignments presented in Table 2, except for the GlcA residue, where ^{13}C and ^{1}H chemical shifts for C-2 and H-2 were exchanged with those of C-4 and H-4, respectively. However, assignment of H-2 of GlcA from the COSY spectrum (Figure S4) was straightforward, thus ascribing this apparent discrepancy to the limits of the CASPER computer program.

2.4. Purification and ^{1}H NMR spectroscopy of the EPOL sample obtained from flocs developed in liquid culture

When KpTs113 was grown in liquid medium, a ring of aggregated cells and matrix grew at the air-liquid interface accompanied also by planktonic growth. Such ring was loosely bound at the test tube

glass walls, and when the growth produced enough mass, it precipitated by gravity at the bottom of the tube, suggesting the formation of multicellular flocs.[6] They were compact and easily collected with a pipette. After purification of the exopolysaccharide from the flocs, a solution of the sample was used to record a ^{1}H NMR spectrum (Figure 2b) which showed that the main polysaccharide in the flocs is identical to the **EPOL Kp113** produced in biofilms on cellulose membranes. In addition to the typical carbohydrate chemical shifts, other resonances in the region 2.5 - 0.0 ppm were detected (data not shown) suggesting the presence of alkyl chains.

In conclusion, *Klebsiella pneumoniae* strain Ts113, isolated from a patient with urinary tract infection, was grown on cellulose membranes to form biofilm, and in liquid medium, where it produced flocs. The polysaccharide fraction isolated from biofilm developed on cellulose membranes resulted to have the same structure of the capsular polysaccharide K24.[17] *Klebsiella* capsular polysaccharides enclose the cells and are also released in the surrounding environment, thus the **EPOL Kp113** may well be the capsular polysaccharide of the KpTs113 strain, and at the same time take part in the biofilm matrix architecture, as found for other strains. In fact, *Klebsiella* capsule was shown to be required for a proper initial coverage of the support and for the development of a mature biofilm matrix.[18] Moreover, **EPOL Kp113** is also the main polysaccharidic component of the flocs, suggesting its involvement in the formation of this type of multicellular aggregate. One of the principal characteristics of biofilms is the adhesion of cells in the first step of biofilm formation. The lack of permanent adhesion to the test tubes walls by KpTs113, accompanied by floc's formation, suggests that the **EPOL Kp113** does have the structural characteristics suitable for the formation of a gel-like matrix, but also that this strain most probably lacks the biosynthesis of other components necessary for the first adhesion event.

3. Experimental

3.1. Bacterial strain, biofilm production and exopolysaccharide purification.

Klebsiella pneumoniae strain Ts113 was isolated from a patient with urinary tract infection. For the production of biofilms, bacteria were grown on cellulose membranes deposited on solid agar medium[19] and in test tubes in liquid medium. Cellulose membranes (Sigma, cut-off 14,000 Da) were cut in circle the size of the Petri dish (90 mm ∅), washed first in a boiling solution of 5% Na_2CO_3 for 15 min and then in boiling water for 15 min, autoclaved and placed over Petri dishes, containing Müller

Hinton (MH) solid medium. The excess of water was removed before seeding the bacteria. Two drops of 10 μL each of an overnight liquid culture of KpTs113 in MH broth were placed on 30 cellulose membranes. After 2 days of incubation at 30 °C, the material from each Petri dish was scraped from the membrane and recovered in 3 - 5 mL of 0.9% NaCl, centrifuged at 48000 g at 4 °C for 20 min, and filter-sterilized (Millipore membranes 0.22 μm). UV spectroscopy showed the absence of proteins and nucleic acids. The solution was dialyzed first against 0.1 M NaCl, then water, taken to pH = 6.8 and recovered by lyophilisation. The polysaccharide was subjected to size exclusion chromatography on a Sephacryl S-300 column. For the production in liquid medium, 50 μL of an overnight liquid culture of KpTs113 in MH broth were used to inoculate 30 test tubes containing 5 mL of MH broth. After incubation at 37°C for five days in static conditions, the bacterial biofilm formed as a thick ring at the liquid air interface and it was loosely attached to the glass. Exopolysaccharides were purified using a modification of the method described by Bales *et al.*:[20] no formaldehyde was used, cells were suspended in 0.1 M NaOH for three hours and no ethanol precipitation was applied. About 9 mg of sample was obtained and half was used to record a proton NMR spectrum.

3.2. General procedures

Analytical GLC was performed on a Perkin-Elmer Autosystem XL gas chromatograph equipped with a flame ionisation detector and using He as carrier gas. An SP2330 capillary column (Supelco, 30 m) was used to separate alditol acetates (temperature program: 200 - 245 °C at 4 °C/min), and partially methylated alditol acetates (temperature program: 150 - 250 °C at 4 °C/min). A HP-1 capillary column (Agilent Technologies, 30 m) was used to separate partially methylated alditol acetates (temperature program: 150 - 245 °C at 2 °C/min), trimethylsilylated methyl glycosides (temperature program: 150 - 280°C at 3 °C/min) and trimethylsilylated (+)-2-butyl glycosides, for the determination of the absolute configuration of the sugar residues,[21] (temperature program: 135 - 240 °C at 1 °C/min). GLC-MS analyses were carried out on an Agilent Technologies 7890A gas chromatograph coupled to an Agilent Technologies 5975C VL MSD. Native and permethylated exopolysaccharides were hydrolysed with 2 M trifluoroacetic acid (TFA) at 125 °C for 1 h. Alditol acetates were prepared as already described.[22] Trimethylsilyl methyl glycosides were obtained by derivatization with the reagent Sylon™ HTP (Sigma) after methanolysis of the polysaccharide with 2 M HCl in methanol at 85 °C for 16 h.[23] Permethylation of the **EPOLs** and oligosaccharides was achieved following the protocol by Harris.[24]

Integration values of the areas of the partially methylated alditol acetates were corrected by the effective carbon response factors.[25]

Size exclusion chromatography of **EPOL Kp113** was performed on a Sephacryl S-300 column (1.6 cm i.d. × 90 cm) using 0.05 M $NaNO_3$ as eluent, and a flow rate of 6 mL/hr. Fractions were collected at 15 min intervals. Elution was monitored using a refractive index detector (WGE Dr. Bures, Lab-Service Analitica), which was connected to a paper recorder and interfaced with a computer via PicoLog software. The central fractions of the eluted peak were pooled together, dialysed and used for linkage analysis and NMR spectroscopy. Oligosaccharides were separated on a Bio Gel P2 column (1.6 cm i.d. × 90 cm) using the same conditions and set up reported above.

*3.3. Smith degradation of the **EPOL Kp113**, purification and ESI-MS analysis of the oligosaccharides obtained*

The **EPOL Kp113** was subjected to Smith degradation.[26] Briefly, 5 mg of the polysaccharide were dissolved in 5 mL of 0.1 M acetate buffer, 32 mg of $NaIO_4$ were added to the solution and the oxidation was let to proceed for 70 hr in the dark at 8°C. After addition of glycerol to react with excess of periodate, reduction of the aldehyde groups was achieved by incubation with $NaBH_4$ at room temperature for 16 h. Excess of borohydride was destroyed with 50% aqueous acetic acid and the solution was dialysed. The recovered material was hydrolysed with 0.5 M TFA for 1 day at room temperature, rotoevaporated to dryness, washed three times with water to remove TFA, taken to pH = 7.1 and once again rotoevaporated to dryness. The sample was named **Kp113 SD** and purified on a Bio Gel P2 column: the fractions of interest were subjected to ESI-MS analysis, after being dialysed using the Spectra/Por® Float-A-Lyzer® G2 devices (membrane cut-off 100 - 500 D, Spectrum Labs).

3.4. NMR experiments

The **EPOL Kp113** was dissolved in water (1 g/L) and sonicated using a Branson sonifier equipped with a microtip at 2.8 Å, in order to decrease its molecular mass. The sample was cooled in an ice bath and sonicated using 5 bursts of 1 min each, separated by 1 min intervals. Polysaccharides were exchanged two times with 99.9% D_2O by lyophilisation and then dissolved in 0.7 mL of 99.96% D_2O. Spectra were recorded on a 500 MHz VARIAN spectrometer operating at 50 °C for **EPOL Kp113** solution and at 60°C for the polysaccharide isolated from flocs. 1D TOCSY were recorded at 50 °C

using 120 ms of spin-lock time. 2D experiments were performed using standard VARIAN pulse sequences and pulsed field gradients for coherence selection when appropriate. HSQC spectra were recorded using 140 Hz (for directly attached ^{1}H - ^{13}C correlations). HMBC experiments were recorded using a coupling constant of 8 Hz (for long range ^{1}H - ^{13}C correlations). TOCSY spectra were acquired using 100 ms spin-lock time and 1.2 s relaxation time. NOESY experiments were recorded with 200 ms mixing time and 1.5 s relaxation time. Chemical shifts are expressed in ppm using acetone as internal reference (2.225 ppm for ^{1}H and 31.07 ppm for ^{13}C). NMR spectra were processed using MestreNova software.

3.5. ESI mass spectrometry

ESI mass spectra were recorded on a Bruker Esquire 4000 ion trap mass spectrometer connected to a syringe pump for the injection of the samples. The instrument was calibrated using a tune mixture provided by Bruker. Oligosaccharides were dissolved in 50% aqueous methanol - 11 mM NH_4OAc; permethylated oligosaccharides were dissolved in a 1:1 chloroform : methanol mixture, 11 mM NH_4OAc. Samples were injected at 180 μL/h. Detection was performed in the positive ion mode.

Acknowledgments

The authors thank Dr. C. Lagatolla (University of Trieste) for the kind gift of *Klebsiella pneumoniae* Ts113 and the University of Trieste (FRA 2011 and FRA 2013) for financial support.

Supplementary data

Supplementary data (Figure S1 – S6, and the Casper report for the top-ranked structure) associated with this article can be found online at

References

1. Pan, Y-J.; Fang, H-C.; Yang, H-C.; Lin, T-L.; Hsieh, P-F.; Tsai, F-C.; Keynan, Y.; Wang, J-T. J. Clin. Microbiol., **2008**, *46*, 2231–2240.
2. Podschun, R.; Ullmann, U. *Clin. Microbiol. Rev.*, **1998**, *11*, 589–603.
3. Campbell, W. N.; Hendrix, E.; Cryz, S.; Cross, A. S. *Clin. Infect. Dis*., **1996**, *23*, 179–181.
4. Domenico, P.; Salo, R. J.; Cross, A. S.; Cunha, B. A. *Infect. Immun.*, **1994**, *62*, 4495–4499.

5. Vuotto, C.; Longo, F.; Balice, M. P.; Donelli, G.; Varaldo, P. E. *Pathogens*, **2014**, *3*, 743–758.
6. Flemming, H-C.; Wingender, J. *Nature Rev. Microbiol.*, **2010**, *8*, 623–633.
7. Carpita, N. C.; Shea E. M. Linkage structure of carbohydrates by gas chromatography-mass spectrometry (GC-MS) of partially methylated alditol acetates. In *Analysis of carbohydrates by GLC and MS*, Biermann, C. J., McGinnis, G. D., Eds; CRC Press: Boca Raton, Florida, 1989, pp 157–216.
8. Vinogradov, E.; Frirdich, E.; MacLean, L. L.; Perry, M. B.; Petersen, B. O.; Duus, J. Ø.; Whitfield, C. *J. Biol. Chem.*, **2002**, *277*, 25070–25081.
9. Aspinall, G. O. Chemical characterization and structure determination of polysaccharides. In *The Polysaccharides*, Aspinall, G. O., Ed; Academic press: New York, 1982, Vol. I, pp 36-131.
10. Winn, A. M.; Wilkinson, S.G. *Carbohydr. Res.*, **1996**, *294*, 109–115.
11. Molinaro, A.; Evidente, A.; Lo Cantore, P.; Iacobellis, N. S.; Bedini, E.; Lanzetta, R.; Parrilli, M. *Eur. J. Org. Chem.*, **2003**, *12*, 2254–2259.
12. Reinhold, V. N.; Reinhold, B. B.; Chan, S. *Methods Enzymol*., 1996, 271, 377–402.
13. Bock, K.; Lundt, I.; Pedersen, C. *Tetrahedron Lett.*, **1973**, *13*, 1037–1040
14. Bock, K.; Pedersen, C. *Adv. Carbohydr. Chem. Biochem.*, **1983**, *41*, 27–66.
15. Lundborg, M.; Widmalm, G. *Anal. Chem*., **2011**, *83*, 1514–1517.
16. Jansson, P.-E.; Stenutz, R.; Widmalm, G. *Carbohydr. Res.*, **2006**, *341*, 1003–1010.
17. Choy, Y-M.; Dutton, G. G. S.; Zanlungo, A. M. *Can. J. Chem.*, **1973**, *51*, 1819–1825.
18. Balestrino D.; Ghigo, J.M.; Charbonnel, N.; Haagensen, J.A.; Forestier, C. *Environ. Microbiol.* **2008**, *10*, 685–701.
19. Merritt, J. H.; Kadouri, D. E.; O'Toole, G. A. *Curr. Protoc. Microbiol.*, **2011**, 1B.1.1–1B.1.18.
20. Bales, P. M.; Renke, E. M.; May, S. L.; Shen, Y.; Nelson, D. C. *PLoS ONE*, **2013**, *8*, e67950.
21. Gerwig, G. J.; Kamerling, J. P.; Vliegenthart, J. F. G. *Carbohydr. Res.*, **1978**, *62*, 349–357.
22. Albersheim, P.; Nevins, D. J.; English, P. D.; Karr, A. *Carbohydr. Res.*, **1967**, *5*, 340–345.
23. Kakehi, K.; Honda, S. Silyl ethers of carbohydrates. In Analysis of carbohydrates by GLC and MS, Biermann, C. J., McGinnis, G. D., Eds; CRC Press: Boca Raton, Florida, 1989, pp 43–85.
24. Harris, P. J.; Henry, R. J.; Blakeney, A. B.; Stone, B. A. *Carbohydr. Res.*, **1984**, *127*, 59–73.
25. Sweet, D. P.; Shapiro, R. H.; Albersheim, P. *Carbohydr. Res.*, **1975**, *40*, 217–225.
26. Goldstein, I. J.; Hay, G. W.; Lewis, B. A.; Smith, F. *Methods Carbohydr. Chem.*, **1965**, *5*, 361–370.
27. Domon, B.; Costello, C. E. *Glycoconjugate J.*, **1988**, *5*, 397–409.

FIGURE LEGENDS

Figure 1: ESI-MS of the permethylated oligosaccharide obtained from Smith degradation of the **EPOL Kp113**. MS^2 of the ion at *m/z* 855.3 (a) and MS^3 of the ion at *m/z* 637.4 (b).

Figure 2: Expansion of the ^1H NMR spectra recorded in D_2O at 50°C of **EPOL Kp113** isolated from biofilm (a) and at 60 °C of the polysaccharide isolated from flocs (b). **A**, **B**, **C**, **D**, and **E** indicate anomeric protons.

Figure 3: Expansion of the HSQC plot recorded in D_2O at 50 °C of **EPOL Kp113** produced in biofilm mode. C - H cross peaks assignments are shown (residues nomenclature is as in Table 2).

Figure 4: Expansion of the NOESY plot recorded in D_2O at 50 °C of **EPOL Kp113** showing inter-residue connectivities. **A**, **B**, **C**, **D**, and **E** as in Table 3.

Table 1 Assignment of ions generated upon fragmentation (MS^2 and MS^3) of **Kp113 SD** oligosaccharide from peak 3 and its perdeuteriomethylated derivative.

Fragmented ions (u) (Composition)	**ions (u)**	**Sequence[a]**	**Ions type[b]**
Kp113-SD oligosaccharide			
687.3	**MS^2 ions (u)**		
(2 Hex, 1 HexA, 1 1,3-Dox)	525.2	HexA-Hex-1,3-Dox	Y_2
	523.2	Hex-HexA-Hex	B_3
	361.1	Hex-HexA	B_2
	349.1	Hex-1,3-Dox	Y_1
permethylated Kp113-SD oligosaccharide			
855.5	**MS^2 ions (u)**		
(2 Hex, 1 HexA, 1 1,3-Dox)	637.2	HexA-Hex-1,3-Dox	Y_2
	419.3	Hex-1,3-Dox	Y_1
637.4	**MS^3 ions (u)**		
(HexA-Hex-1,3-Dox)	419.1	Hex-1,3-Dox	Y_1
	215.1	1,3-Dox	Y_0

[a] all ions are sodium adducts; 1,3-Dox stands for 1,3 dioxolane

[b] According to the fragmentation proposed by Domon and Costello[27]

Table 2

^{1}H and ^{13}C chemical shift assignments of the **EPOL Kp113** produced by *K. pneumoniae* strain Ts113

Residues[a]	**Nucleus**	**Chemical shifts (ppm)**[b]					
		1	**2**	**3**	**4**	**5**	**6**
A [177.69]	**^{1}H**	5.45	4.06	3.93	3.72	3.96	nd
→2)-α-D-Man*p*-(1→	**^{13}C**	100.39	79.94	71.00	67.81	73.70	nd
B [177.69]	**^{1}H**	5.44	3.80	4.03	3.77	4.18	-
→2,4)-α-D-Glc*p*A-(1→	**^{13}C**	100.39	81.12	71.18	81.14	72.79	176.32
C [172.53]	**^{1}H**	5.00	4.20	3.92	3.88	3.77	nd
→3)-α-D-Man*p*-(1→	**^{13}C**	103.17	70.57	80.47	66.62	73.97	nd
D [167.60]	**^{1}H**	4.69	3.41	3.64	3.57	3.47	3.77 - 3.91
→3)-β-D-Glc*p*-(1→	**^{13}C**	104.73	73.03	83.01	70.12	75.95	61.54
E [163.18]	**^{1}H**	4.65	3.99	3.63	3.58	3.38	
β-D-Man*p*-(1→	**^{13}C**	100.65	71.39	73.59	67.59	77.20	nd

[a] $^{1}J_{C1,H1}$ in square brackets.

[b] Chemical shifts are given relative to internal acetone (2.225 ppm for ^{1}H and 31.07 ppm for ^{13}C).

Table 3: Inter- and intra-residues NOE contacts of the anomeric protons of **EPOL Kp113**

Residue	NOE contact (ppm)[a]	assignment
A1	5.00	**C**1
	4.06	**A**2
	3.64	**D**3
	3.57	**D**4
	3.77	**D**6
B1	4.69	**D**1
	4.20	**C**2
	3.92	**C**3
	3.88	**C**4
C1	5.45	**A**1
	4.20	**C**2
	4.06	**A**2
	3.93	**A**3
D1	5.45	**A**1
	3.80	**B**2
	3.48	**D**5
E1	3.99	**E**2
	3.78	**B**4
	3.63	**E**3
	3.38	**E**5

[a] Chemical shifts are given relative to internal acetone (2.225 ppm for ^{1}H).

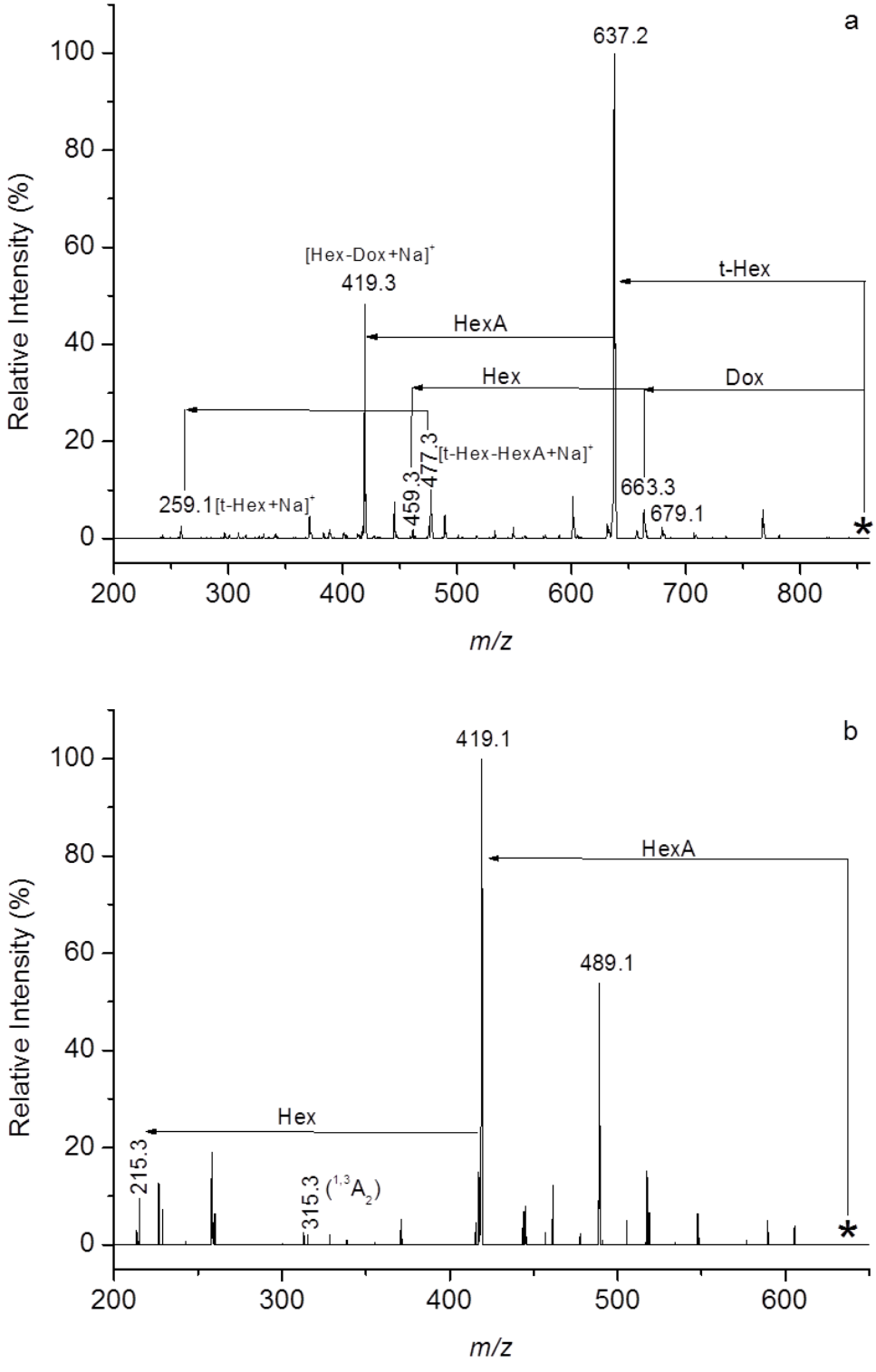
a
637.2
[Hex-Dox+Na]+
419.3
t-Hex
HexA
Hex
Dox
[t-Hex-HexA+Na]+
477.3
459.3
663.3
679.1
259.1[t-Hex+Na]+
*
Relative Intensity (%)
m/z
b
419.1
HexA
489.1
Hex
215.3
315.3 (1,3A2)
*
Relative Intensity (%)
m/z

Figure 1

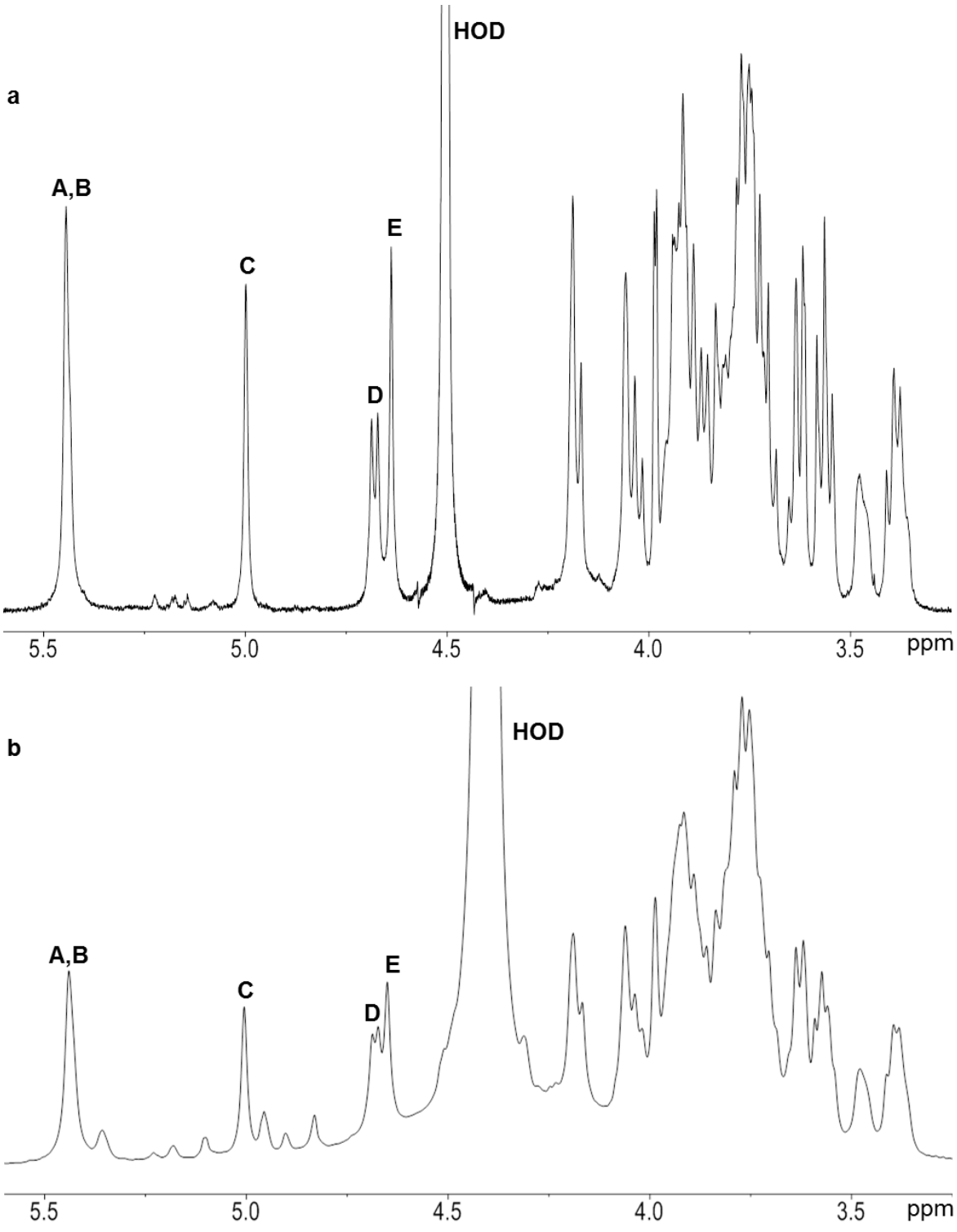

Figure 2

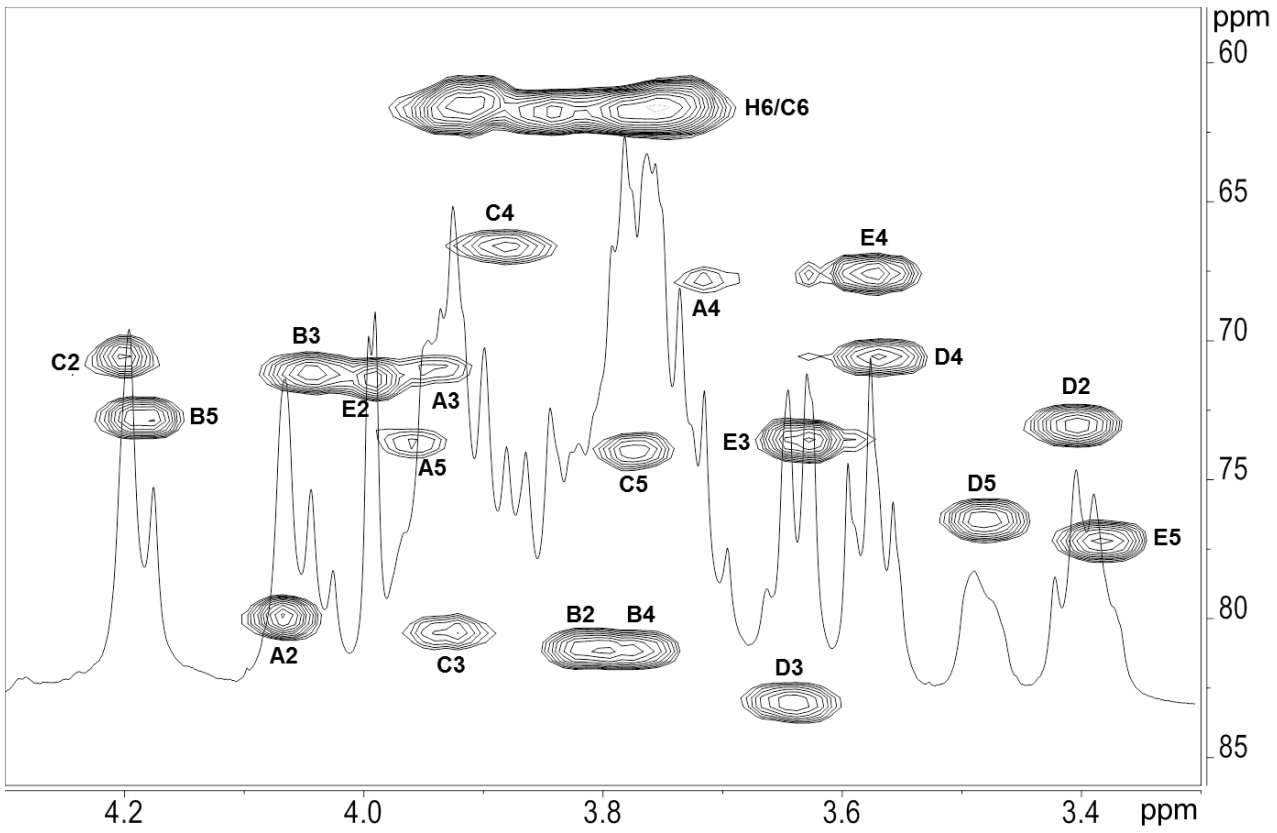
ppm
60
65
70
75
80
85
H6/C6
C4
E4
A4
B3
C2
D4
D2
B5
E2
A3
E3
A5
C5
D5
E5
B2
B4
A2
C3
D3
4.2
4.0
3.8
3.6
3.4
ppm

Figure 3

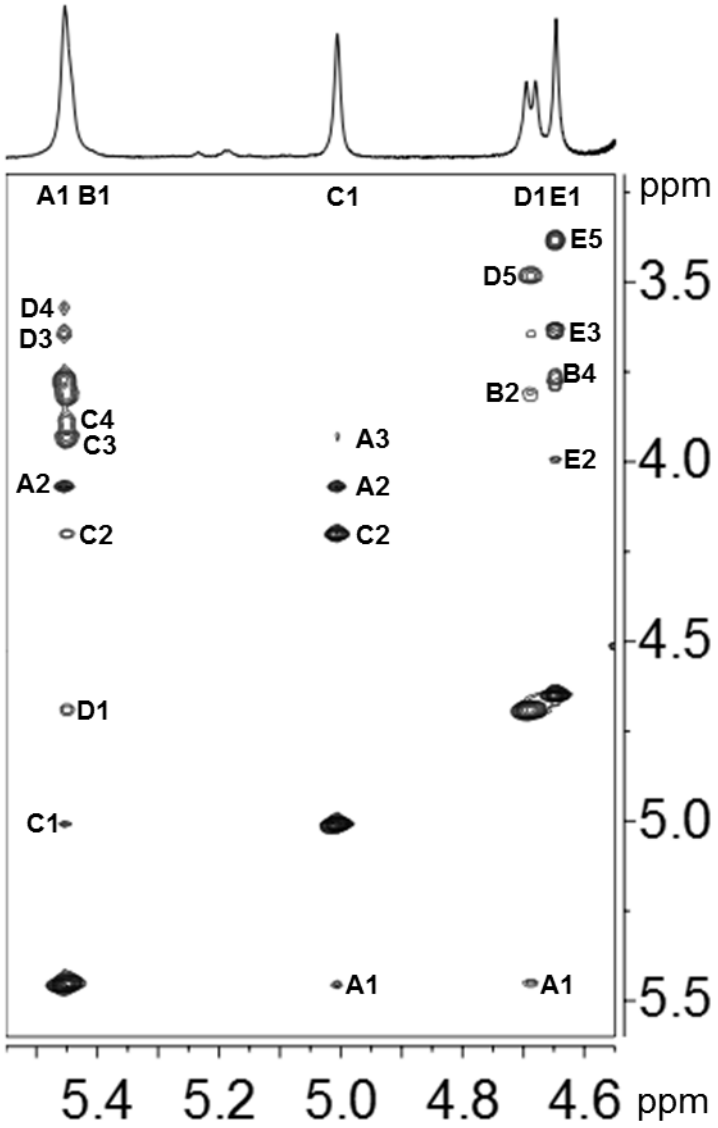
A1 B1
C1
D1 E1
E5
D5
D4
D3
E3
B4
B2
C4
C3
A3
E2
A2
A2
C2
C2
D1
C1
A1
A1
ppm
3.5
4.0
4.5
5.0
5.5
5.4
5.2
5.0
4.8
4.6
ppm

Figure 4

GRAPHICAL ABSTRACT

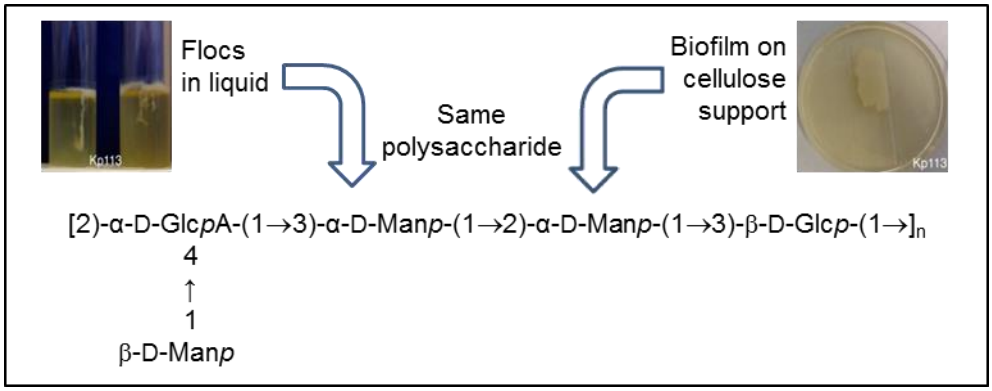

HIGHLIGHTS

- *Klebsiella pneumoniae* strain Ts113 was isolated from a urinary tract infection
- KpTs113 was grown on cellulose membranes to form biofilms
- KpTs113 in liquid medium produced flocs
- Biofilms on cellulose membranes and flocs contained the same polysaccharide
- The polysaccharide produced by KpTs113 is identical to that of *Klebsiella* K24

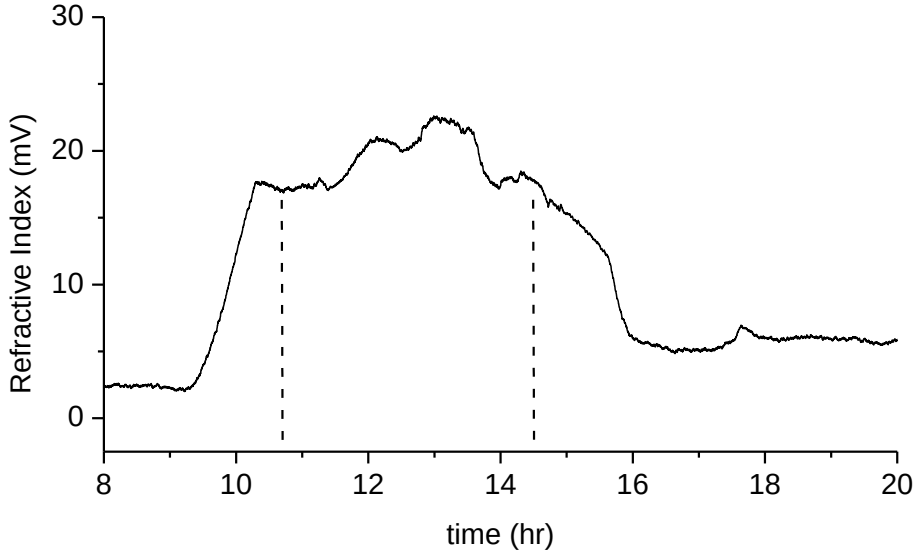

Figure S1: Sephacryl S-300 size exclusion chromatography elution profile of **EPOL Kp113**. Fractions within dashed lines were pooled together and used for structural studies.

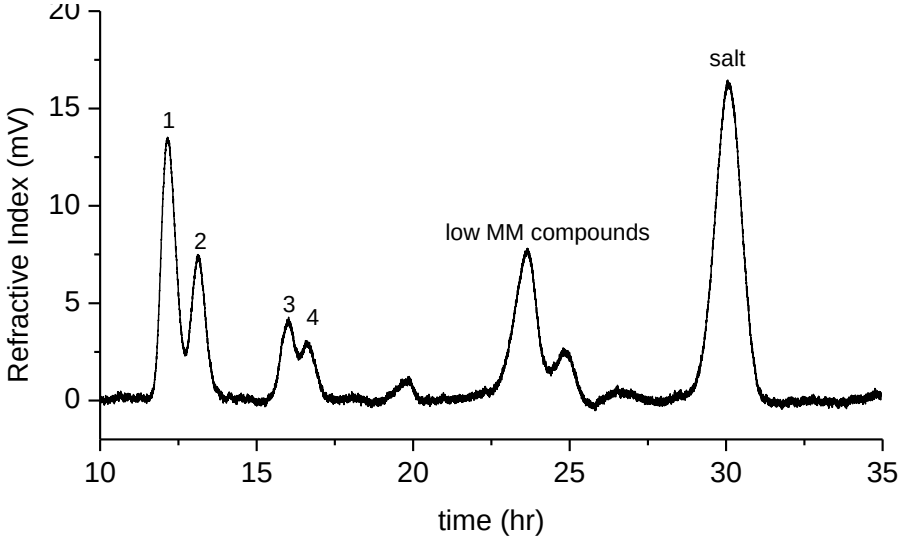

Figure S2: Bio Gel P2 size exclusion chromatography elution profile of **Kp113-SD** sample. Peaks were analysed by ESI-MS and peak 3 was shown to contain the oligosaccharide of interest Hex-HexA-Hex-Dox (Dox = 1,3-dioxolane), expected to be recovered after Smith degradation. Peaks 1 and 2 contained saccharides of higher size, deriving from incomplete hydrolysis, and peak 4 contained di- and trisaccharides.

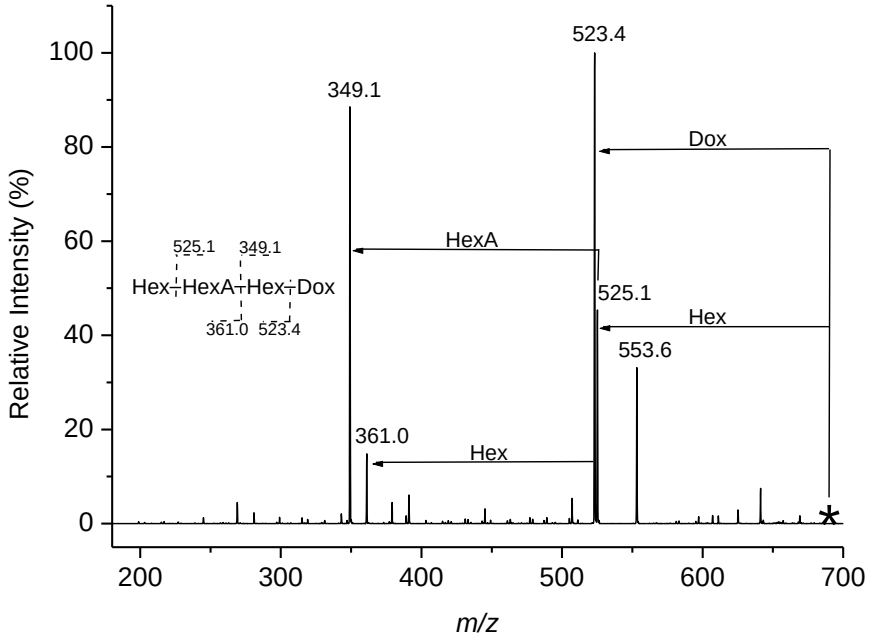

Figure S3: ESI-MS fragmentation of the parent ion at 687.2 *m/z* and deduced fragmentation scheme.

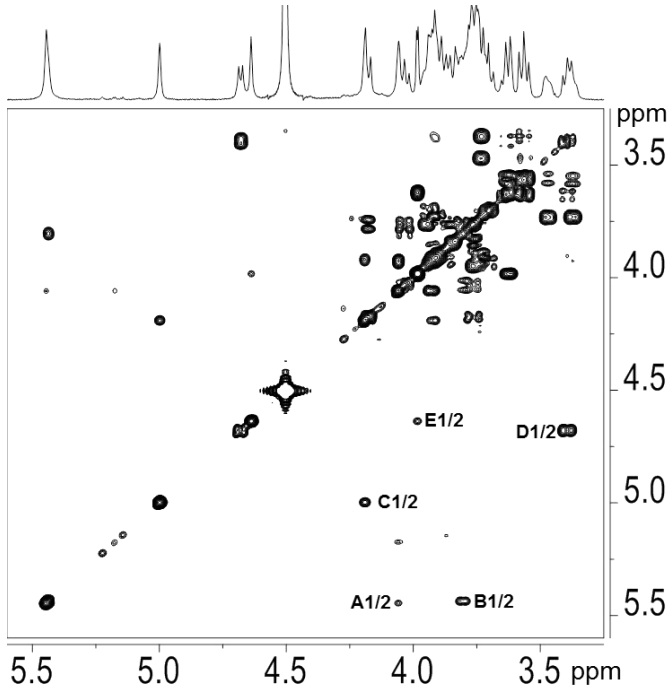

Figure S4: COSY expansion recorded in D_2O at 50°C of a solution of **EPOL Kp113** produced in biofilm mode. Some correlations are indicated (see Table 2).

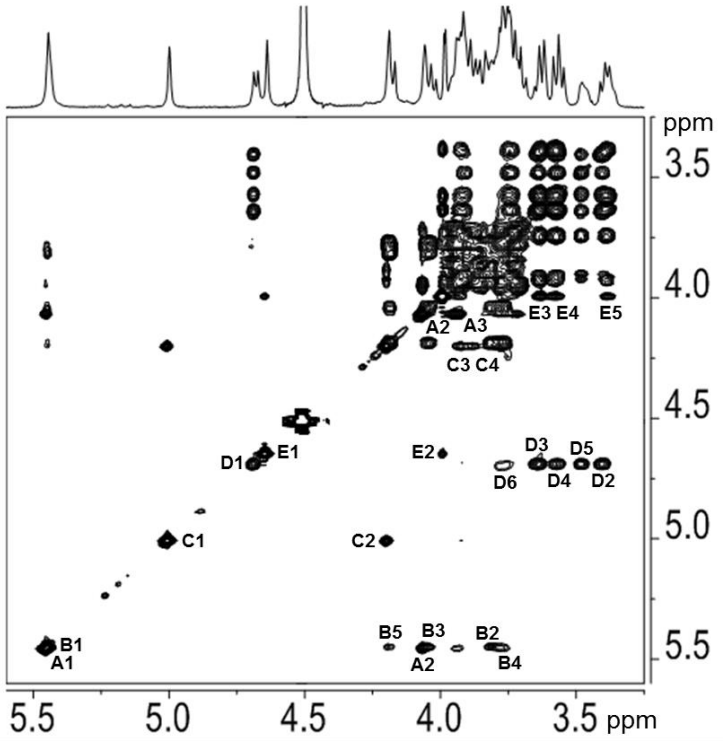

Figure S5: TOCSY expansion recorded in D_2O at 50°C of a solution of **EPOL Kp113** produced in biofilm mode. Some correlations are indicated (see Table 2).

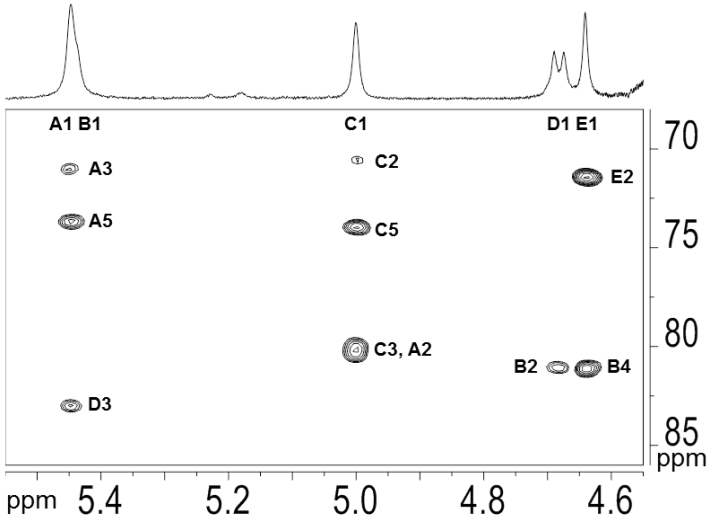

Figure S6: HMBC expansion recorded in D_2O at 50°C of a solution of **EPOL Kp113** produced in biofilm mode. Intra- and inter-residue connectivities are shown (see Table 3).

CASPER program output of the ten best structures for Kp113 EPOL repeating unit

Proposed structures

1. →2)[β-D-Man-(1→4)]α-D-GlcA-(1→3)-α-D-Man-(1→2)-α-D-Man-(1→3)-β-D-Glc-(1→, δ_{Rel}=1.00
   δ_{CH}=2.56 (0.08) Assignment completeness: 100.0%
2. →2)[β-D-Man-(1→4)]α-D-GlcA-(1→2)-α-D-Man-(1→3)-α-D-Man-(1→3)-β-D-Glc-(1→, δ_{Rel}=1.16
   δ_{CH}=2.96 (0.09) Assignment completeness: 100.0%
3. →4)[α-D-Man-(1→2)-α-D-Man-(1→3)-β-D-Glc-(1→2)]α-D-GlcA-(1→3)-β-D-Man-(1→, δ_{Rel}=1.25
   δ_{CH}=3.19 (0.10) Assignment completeness: 100.0%
4. →4)[β-D-Man-(1→3)-α-D-Man-(1→2)-α-D-Man-(1→3)-β-D-Glc-(1→2)]α-D-GlcA-(1→, δ_{Rel}=1.27
   δ_{CH}=3.26 (0.10) Assignment completeness: 100.0%
5. →4)[β-D-Man-(1→2)]α-D-GlcA-(1→3)-α-D-Man-(1→2)-α-D-Man-(1→3)-β-D-Glc-(1→, δ_{Rel}=1.29
   δ_{CH}=3.30 (0.10) Assignment completeness: 100.0%
6. →2)[α-D-Man-(1→3)-β-D-Man-(1→4)]α-D-GlcA-(1→2)-α-D-Man-(1→3)-β-D-Glc-(1→, δ_{Rel}=1.30
   δ_{CH}=3.33 (0.10) Assignment completeness: 100.0%
7. →2)[α-D-Man-(1→3)-β-D-Man-(1→3)]α-D-GlcA-(1→2)-α-D-Man-(1→3)-β-D-Glc-(1→, δ_{Rel}=1.31
   δ_{CH}=3.35 (0.10) Assignment completeness: 100.0%
8. →2)[β-D-Man-(1→3)]α-D-GlcA-(1→3)-α-D-Man-(1→2)-α-D-Man-(1→3)-β-D-Glc-(1→, δ_{Rel}=1.32
   δ_{CH}=3.37 (0.10) Assignment completeness: 100.0%
9. →3)[α-D-Man-(1→2)-α-D-Man-(1→3)-β-D-Glc-(1→2)]α-D-GlcA-(1→3)-β-D-Man-(1→, δ_{Rel}=1.32
   δ_{CH}=3.37 (0.10) Assignment completeness: 100.0%
10. →4)[β-D-Man-(1→2)-α-D-Man-(1→3)-α-D-Man-(1→3)-β-D-Glc-(1→2)]α-D-GlcA-(1→, δ_{Rel}=1.35
    δ_{CH}=3.45 (0.10) Assignment completeness: 100.0%

Figure S7: the CASPER program output of the ten best structures determined for the repeating unit of the **EPOL Kp113**. Assignment completeness gives the fraction of calculated chemical shifts that could be assigned to an experimental signal. $\delta_{Rel} = (0.1\times\delta_C + 5.0\times\delta_{CH} + 1.0\times\delta_{HH})$/Assignment Completeness, normalized so that the top-ranked structure has a δ_{Rel}=1.00.

CASPER report for the top-ranked structure of Figure S6

Calculated ^{13}C and ^{1}H chemical shifts

Structure

→2)[β-D-Man^{v}(1→4)]α-D-GlcA^{iv}(1→3)α-D-Man^{iii}(1→2)α-D-Man^{ii}(1→3)β-D

→3)β-D-Glc^{i}(1→	1	2	3	4	5	6	6
Expected Calc. Error: 4.61	104.82	73.14	83.15	70.64	76.67	61.29	
	4.70	3.44	3.69	3.61	3.49	3.76	3.92
→2)α-D-Man^{ii}(1→	1	2	3	4	5	6	6
Expected Calc. Error: 3.36	100.08	79.29	71.12	67.89	73.80	61.93	
	5.47	4.10	3.99	3.78	3.97	3.79	3.88
→3)α-D-Man^{iii}(1→	1	2	3	4	5	6	6
Expected Calc. Error: 4.72	102.39	70.55	79.30	66.83	74.02	61.72	
	5.07	4.27	4.02	3.91	3.79	3.79	3.89
→2,4)α-D-GlcA^{iv}(1→	1	2	3	4	5	6	
Expected Calc. Error: 4.27	100.68	81.18	70.80	81.76	71.79	176.69	
	5.48	3.78	4.14	3.84	4.17		
β-D-Man^{v}(1→	1	2	3	4	5	6	6
Expected Calc. Error: 0.85	100.92	71.42	73.80	67.63	77.23	61.86	
	4.72	4.04	3.63	3.60	3.40	3.74	3.92

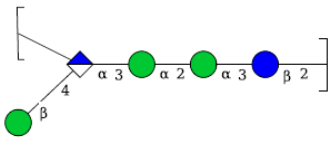

Assignment of ^{13}C, ^{1}H resonances

Experimental	Calculated	Expt-Calc	Assignment
104.73 - 4.69	104.82 - 4.70	0.02	β-D-Glc^{i} - 1
103.17 - 5.00	102.39 - 5.07	0.17	α-D-Man^{iii} - 1
100.65 - 4.65	100.92 - 4.72	0.09	β-D-Man^{v} - 1
100.39 - 5.45	100.68 - 5.48	0.06	α-D-GlcA^{iv} - 1
100.39 - 5.44	100.08 - 5.47	0.07	α-D-Man^{ii} - 1
83.01 - 3.64	83.15 - 3.69	0.05	β-D-Glc^{i} - 3
81.12 - 3.80	81.76 - 3.84	0.13	α-D-GlcA^{iv} - 4
81.14 - 3.77	81.18 - 3.78	0.01	α-D-GlcA^{iv} - 2
80.47 - 3.92	79.30 - 4.02	0.25	α-D-Man^{iii} - 3
79.94 - 4.06	79.29 - 4.10	0.14	α-D-Man^{ii} - 2
77.20 - 3.38	77.23 - 3.40	0.03	β-D-Man^{v} - 5
75.95 - 3.47	76.67 - 3.49	0.15	β-D-Glc^{i} - 5
73.97 - 3.77	74.02 - 3.79	0.02	α-D-Man^{iii} - 5
73.70 - 3.96	73.80 - 3.97	0.02	α-D-Man^{ii} - 5
73.59 - 3.63	73.80 - 3.63	0.04	β-D-Man^{v} - 3
73.03 - 3.41	73.14 - 3.44	0.04	β-D-Glc^{i} - 2
72.79 - 4.18	71.79 - 4.17	0.20	α-D-GlcA^{iv} - 5
71.39 - 3.99	71.42 - 4.04	0.05	β-D-Man^{v} - 2
71.00 - 3.93	71.12 - 3.99	0.06	α-D-Man^{ii} - 3
71.18 - 4.03	70.80 - 4.14	0.14	α-D-GlcA^{iv} - 3
70.12 - 3.57	70.64 - 3.61	0.11	β-D-Glc^{i} - 4
70.57 - 4.20	70.55 - 4.27	0.07	α-D-Man^{iii} - 2
67.81 - 3.72	67.89 - 3.78	0.06	α-D-Man^{ii} - 4
67.59 - 3.58	67.63 - 3.60	0.02	β-D-Man^{v} - 4
66.62 - 3.88	66.83 - 3.91	0.05	α-D-Man^{iii} - 4
61.75 - 3.84	61.93 - 3.88	0.05	α-D-Man^{ii} - 6
61.75 - 3.84	61.93 - 3.79	0.06	α-D-Man^{ii} - 6'
61.60 - 3.75	61.86 - 3.92	0.17	β-D-Man^{v} - 6
61.60 - 3.75	61.86 - 3.74	0.05	β-D-Man^{v} - 6'
61.53 - 3.92	61.72 - 3.89	0.05	α-D-Man^{iii} - 6
61.53 - 3.92	61.72 - 3.79	0.13	α-D-Man^{iii} - 6'
61.53 - 3.92	61.29 - 3.92	0.05	β-D-Glc^{i} - 6
61.53 - 3.92	61.29 - 3.76	0.17	β-D-Glc^{i} - 6'
Error=2.56 (0.09/signal), RMS error=0.10.			

Assigned experimental ^{13}C and ^{1}H chemical shifts

Structure

→2)[β-D-Man^{v}(1→4)]α-D-GlcA^{iv}(1→3)α-D-Man^{iii}(1→2)α-D-Man^{ii}(1→3)β-D-Glc^{i}(1→

→3)β-D-Glc^{i}(1→	1	2	3	4	5	6	6
^{13}C Error: 1.82. ^{1}H Error: 0.32.	104.73	73.03	83.01	70.12	75.95	61.53	
	4.69	3.41	3.64	3.57	3.47	3.92	3.92
→2)α-D-Man^{ii}(1→	1	2	3	4	5	6	6
^{13}C Error: 1.44. ^{1}H Error: 0.27.	100.39	79.94	71.00	67.81	73.70	61.75	
	5.44	4.06	3.93	3.72	3.96	3.84	3.84
→3)α-D-Man^{iii}(1→	1	2	3	4	5	6	6
^{13}C Error: 2.42. ^{1}H Error: 0.45.	103.17	70.57	80.47	66.62	73.97	61.53	
	5.00	4.20	3.92	3.88	3.77	3.92	3.92
→2,4)α-D-GlcA^{iv}(1→	1	2	3	4	5	6	
^{13}C Error: 2.35. ^{1}H Error: 0.20.	100.39	81.14	71.18	81.12	72.79	n.d.	
	5.45	3.77	4.03	3.80	4.18		
β-D-Man^{v}(1→	1	2	3	4	5	6	6
^{13}C Error: 0.84. ^{1}H Error: 0.35.	100.65	71.39	73.59	67.59	77.20	61.60	
	4.65	3.99	3.63	3.58	3.38	3.75	3.75